Article

Cell Systems

Noisy Response to Antibiotic Stress Predicts Subsequent Single-Cell Survival in an Acidic Environment

Graphical Abstract

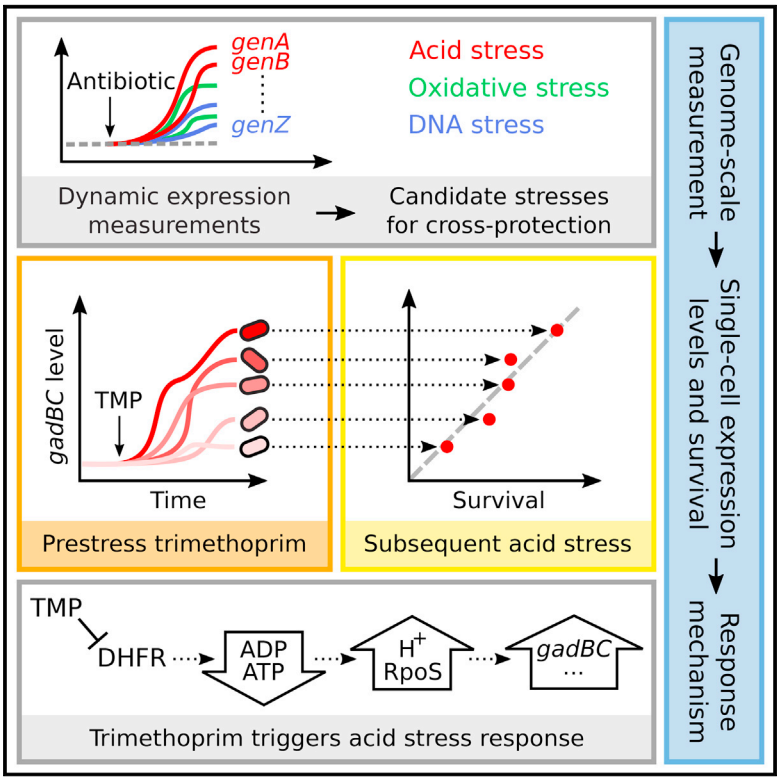

Authors

Karin Mitosch, Georg Rieckh, Tobias Bollenbach

Correspondence

t.bollenbach@uni-koeln.de

In Brief

Stress response programs induced by antibiotics, identified by genome-wide measurements of expression dynamics, are shown to cross-protect bacteria from subsequent environmental stress. In particular, the noisy expression level of a major acid stress operon, induced by folate synthesis inhibition, explains the differential survival of single cells in an acidic environment.

Highlights

- Antibiotics induce diverse and temporally structured gene expression changes in *E. coli*
- Acid stress response to trimethoprim protects bacteria from subsequent HCl challenge
- Noisy expression of a major acid stress operon (*gadBC*) predicts survival of single cells
- Depletion of adenine nucleotides underlies this cross-protection effect

Mitosch et al., 2017, Cell Systems *4*, 393–403
April 26, 2017
http://dx.doi.org/10.1016/j.cels.2017.03.001

Cell Systems
Article

Noisy Response to Antibiotic Stress Predicts Subsequent Single-Cell Survival in an Acidic Environment

Karin Mitosch,[1] Georg Rieckh,[1,2] and Tobias Bollenbach[1,3,4,*]
[1]IST Austria, 3400 Klosterneuburg, Austria
[2]Division of Biological Sciences, University of California at San Diego, La Jolla, CA 92093, USA
[3]Institute for Theoretical Physics, University of Cologne, 50937 Cologne, Germany
[4]Lead Contact
*Correspondence: t.bollenbach@uni-koeln.de
http://dx.doi.org/10.1016/j.cels.2017.03.001

SUMMARY

Antibiotics elicit drastic changes in microbial gene expression, including the induction of stress response genes. While certain stress responses are known to "cross-protect" bacteria from other stressors, it is unclear whether cellular responses to antibiotics have a similar protective role. By measuring the genome-wide transcriptional response dynamics of *Escherichia coli* to four antibiotics, we found that trimethoprim induces a rapid acid stress response that protects bacteria from subsequent exposure to acid. Combining microfluidics with time-lapse imaging to monitor survival and acid stress response in single cells revealed that the noisy expression of the acid resistance operon *gadBC* correlates with single-cell survival. Cells with higher *gadBC* expression following trimethoprim maintain higher intracellular pH and survive the acid stress longer. The seemingly random single-cell survival under acid stress can therefore be predicted from *gadBC* expression and rationalized in terms of GadB/C molecular function. Overall, we provide a roadmap for identifying the molecular mechanisms of single-cell cross-protection between antibiotics and other stressors.

INTRODUCTION

Microbes regularly encounter harsh environmental conditions. Both general and specific stress response programs help them survive the current stress; these responses may also protect them against subsequent higher levels of the same stress (Begley et al., 2002; Berry and Gasch, 2008; Goodson and Rowbury, 1989) or against different stresses (Al-Nabulsi et al., 2015; Battesti et al., 2011; Jenkins et al., 1988; Leyer and Johnson, 1993; McMahon et al., 2007; Wang and Doyle, 1998). Certain stress response programs are also specifically coupled, suggesting frequent co-occurrence of the corresponding stressors in the environment over the bacterium's evolutionary history (Mitchell et al., 2009; Tagkopoulos et al., 2008). Antibiotics, i.e., small molecules that inhibit or kill bacteria by specifically targeting essential cellular processes, trigger massive and complex changes in metabolism and global gene expression (Belenky et al., 2015; Brazas and Hancock, 2005; Goh et al., 2002; Kwon et al., 2010), including the induction of specific stress response genes. For most antibiotics-induced gene expression changes it is, however, unclear if they can change the microbes' ability to survive environmental changes such as low pH, oxidative stress, or heat.

Such environmental stresses and their sudden fluctuations are commonplace challenges for commensal and pathogenic bacteria. For example, bacteria entering the mammalian stomach suddenly experience an acidic environment with pH values as low as pH 2 (Weinstein et al., 2013). Antibiotics are a similarly widespread impediment for bacterial growth: they are often produced by other microbes in the environment (Martín and Liras, 1989; Waksman, 1961) and their occurrence is further increased by their use in treating human infections and in agriculture with its resultant contaminations of water and soil (Andersson and Hughes, 2014). It is therefore relevant to study the combined effects of antibiotics and environmental stressors on bacteria. In particular, the bacterial stress response programs triggered by antibiotics can indicate changes in bacterial susceptibility and new vulnerabilities to specific environmental stressors.

Most stress response mechanisms were elaborated at the population level. However, the expression of stress response genes tends to be highly variable from cell to cell (Locke et al., 2011; Newman et al., 2006; Silander et al., 2012), which can result in different phenotypes at the single-cell level and varying probabilities of an individual's survival (El Meouche et al., 2016; Sánchez-Romero and Casadesús, 2014). For example, in response to low concentrations of streptomycin, the expression level of a heat shock promoter in *E. coli* increased and became more variable and negatively correlated with survival (Ni et al., 2012). In another study, *Salmonella* bacteria variably expressed virulence genes in response to spent growth medium (Arnoldini et al., 2014); those individual bacteria that most highly expressed the virulence genes had a lower growth rate and a more than 1,000-fold higher probability to survive clinically relevant ciprofloxacin concentrations (Arnoldini et al., 2014). This is an example of "cross-protection": adaptation to one stressful environment (spent growth medium) provides a fitness benefit when cells are exposed to a second stressor (antibiotics).

Table 1. Antibiotics Used in This Study

Antibiotic	Abbreviation	Mechanism of Action	Concentration (μg/mL)
Trimethoprim	TMP	Folate synthesis inhibition	0.5 (1.0, 5.0)
Tetracycline	TET	Ribosome 30S inhibition	0.7
Nitrofurantoin	NIT	Nitro radicals	4.0
Chloramphenicol	CHL	Ribosome 50S inhibition	1.0

Concentrations were adjusted such that they led to a growth rate inhibition of 40%–50% (Figure S1A); TMP 1 μg/mL reduced growth rate to ~38% and TMP 5 μg/mL to ~15%.

Here, we ask if cross-protection can occur in the opposite direction: can antibiotics-induced gene expression changes provide protection against environmental stressors? We are also interested in disentangling the molecular events that lead to such cross-protection and in the fundamental question of whether the heterogeneous single-cell survival under those stressors can be predicted from the gene expression level of stress response genes in individual cells. To identify antibiotics-induced gene expression changes that might cross-protect from different stressors, we measured the genome-wide transcriptional regulation dynamics in response to four antibiotics using a fluorescent reporter library. We found that trimethoprim (TMP) triggered a particularly strong and fast acid stress response, which indeed led to cross-protection from extreme acid stress. We found that the variable expression of the acid resistance operon *gadBC* predicted single-cell survival under acid stress. Survival of single cells also correlated with the intracellular pH of individual cells; this observation directly connects the function of TMP-induced GadB/C in pH homeostasis to survival following environmental stress. We demonstrate that acid stress response induced by TMP results from the intracellular depletion of adenine nucleotides, a downstream effect of TMP. The cross-protection between TMP and acid stress presented here shows how antibiotics can increase bacterial fitness in changing environments.

RESULTS

Antibiotics Trigger a Temporally Structured Gene Expression Program, Including a Rapid Acid Stress Response under TMP

To identify which potentially cross-protecting stress responses are triggered by different antibiotics we developed a protocol to measure genome-wide gene expression in response to antibiotic treatment at high time-resolution. We used the antibiotics TMP, tetracycline (TET), nitrofurantoin (NIT), and chloramphenicol (CHL), representing diverse modes of action (Table 1). We maintained bacterial cultures of a genome-wide promoter-GFP library (Zaslaver et al., 2006) in exponential growth by four successive 10-fold dilutions using a robotic liquid handling system (Figures 1A and 1B; STAR Methods). Antibiotics were added after ~10 hr; concentrations were tuned to result in 40%–50% growth inhibition (Figure S1A). This protocol enabled us to reliably quantify the expression changes of ~1,000 promoters at a temporal resolution of ~25 min (see STAR Methods for details; dataset in Table S1).

We tested how strongly and how fast various promoters responded to antibiotics. Response times, which were measured as the time until half maximum expression level change was reached (Figure 1C; STAR Methods), ranged from tens of minutes to several hours (Figure 1D), considerably exceeding the generation time (~100 min in our conditions). While only ~5% of the ~1,000 tested library promoters responded to CHL, about 20% of promoters were up- or downregulated by more than 2-fold for TMP and TET (Figure 1D). In an unstressed control, using the same dilution protocol, only 3% of all promoters exceeded the 2-fold threshold. When applying a >3-fold threshold, we detected 5% (TMP), 6% (TET), and 3% (NIT) differentially regulated promoters, which is comparable with previous results reporting that ~5% of genes have a differential expression of >3-fold for different antibiotics (Goh et al., 2002). Based on these high numbers, we hypothesized that TMP, TET, and NIT might cross-protect from stressors which induce similar protective responses as these antibiotics.

Many general and specific stress response promoters were strongly up- or downregulated. Specifically, NIT and TET triggered an early oxidative stress response, while TMP and NIT induced a delayed SOS response (Bryant and McCalla, 1980; Lewin and Amyes, 1991; Sangurdekar et al., 2011). Promoters from the glutamate-dependent acid resistance system, which provides protection at extremely low pH (Lin et al., 1996), showed particularly strong changes: they were downregulated under NIT (10.9-fold enrichment in the downregulated promoters, $p = 6.7 \times 10^{-7}$; hypergeometric test) but rapidly and transiently upregulated under TMP (4.3-fold enrichment in the upregulated promoters, $p = 1.4 \times 10^{-3}$; Figure 1D and 1E). This pulse of acid stress responsive transcription coincided with an initially more pronounced growth rate drop under TMP (Figure 1B). The upregulation of acid stress promoters was not detectable when using a simpler stress protocol without dilutions in which TMP was present right from the start of the experiment; overall, however, many differentially regulated promoters were also captured in the simpler protocol (Figure S1B).

Most acid stress response genes are regulated by the general stress sigma factor RpoS and activated in stationary phase (De Biase et al., 1999; Seo et al., 2015). Further, pH downshift or overexpression of the acid stress regulator GadX increases RpoS levels (Hommais et al., 2004). We observed that promoters regulated by the general stress sigma factor RpoS were also upregulated by TMP (2.3-fold enrichment in the upregulated promoters, $p = 1.6 \times 10^{-4}$; Figure 1D). Across the antibiotics tested, this response is specific to TMP pre-treatment; these genes are mostly repressed by NIT (2.8-fold enrichment in downregulated promoters, $p = 2.9 \times 10^{-3}$; Figure 1D). Note, however, that detection of the response times for downregulated genes was less sensitive: as the used GFP is stable (Zaslaver et al., 2006), its concentration can maximally decrease at the rate of dilution due to growth. Together, these data confirm the close interdependence between the acid and the general RpoS-mediated stress response (Weber et al., 2005).

The induction of the glutamate-dependent acid resistance system by TMP was unexpected since TMP does not acidify the medium, is unlikely to act as a potent acid ($pK_a \sim 7$; Qiang

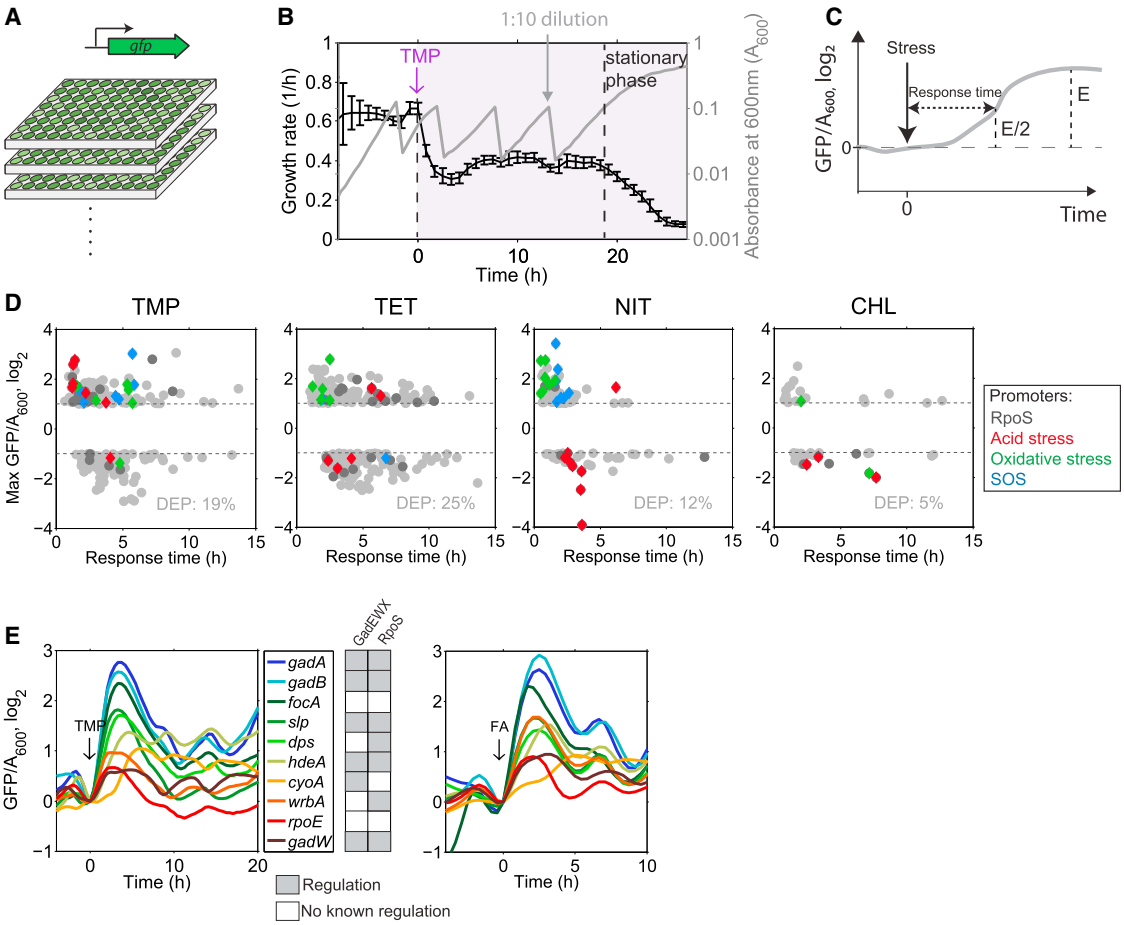

Figure 1. Dynamic Measurements of Genome-wide Transcriptional Response to Antibiotics Reveal a Rapid, Strong Acid Stress Response Pulse Triggered by TMP

(A) Schematic of the genome-wide promoter-GFP library (Zaslaver et al., 2006).

(B) Growth rate (black line, error bars are SD from all reporter strains) and absorbance (A_{600}) (gray line) of one reporter strain (P_{aroH}-*gfp*) over time in response to sustained TMP stress, suddenly added at $t = 0$.

(C) Schematic illustrating response time determined as the time until half maximum expression on a $\log_2$ scale.

(D) Genome-wide maximal gene expression changes and response times upon sudden addition of different antibiotics (TMP, TET, NIT, and CHL). Shown are all promoters that changed expression by >2-fold; dark gray dots are RpoS-regulated promoters, red diamonds are GadEWX-regulated, green diamonds are SoxS or OxyR-regulated and blue diamonds are LexA-regulated. DEP is the percentage of differentially expressed promoters (changing >2-fold). Dataset with genome-wide gene expression changes over time can be found in Table S1.

(E) Normalized gene expression over time for selected acid stress and RpoS-regulated promoters in response to sustained TMP stress (0.5 μg/mL) or formic acid (FA) stress titrated to pH 6.4, suddenly added at $t = 0$. The table shows known transcriptional regulation (gray square) or no known regulation (white square) by GadEWX or RpoS, according to (Keseler et al., 2013; Seo et al., 2015). See also Figure S1.

and Adams, 2004), and its mechanism of action (inhibition of folate synthesis) is not obviously related to intracellular acidification. As a first step toward understanding how TMP induces the acid stress response, we asked whether this response was part of the general stress response induced by RpoS or if it was activated more specifically and independently of RpoS. To this end, we measured the expression of a key acid stress promoter, P_{gadB}, following TMP treatment in an *rpoS* deletion strain (Baba et al., 2006). During acid stress P_{gadB} controls the expression of one of the glutamate decarboxylases in *E. coli*, GadB, and the glutamate:4-aminobutyrate antiporter GadC in an RpoS-dependent manner. The presence of both enzymes is essential for survival at low external pH (Castanie-Cornet et al., 1999; Richard and Foster, 2004): GadB catalyzes the proton-consuming decarboxylation on glutamate and GadC exchanges the product γ-aminobutyric acid for glutamate, thereby increasing intracellular pH (Hersh et al., 1996; Tsai et al., 2013). GadB has a homolog, GadA, with highly similar regulation and redundant function (Keseler et al., 2013). In contrast, there is no homolog for GadC in *E. coli* which renders a *ΔgadC* strain extremely sensitive to acid (Castanie-Cornet et al., 1999). We observed that this system is activated by TMP independently of RpoS: the basal expression of *gadBC* was 6-fold lower in the Δ*rpoS* strain but this strain still upregulated *gadBC* by 7-fold in response to TMP (compared with 13-fold in the wild-type, Figure S1C). Thus, we conclude that while RpoS is needed for the basal expression of *gadBC*

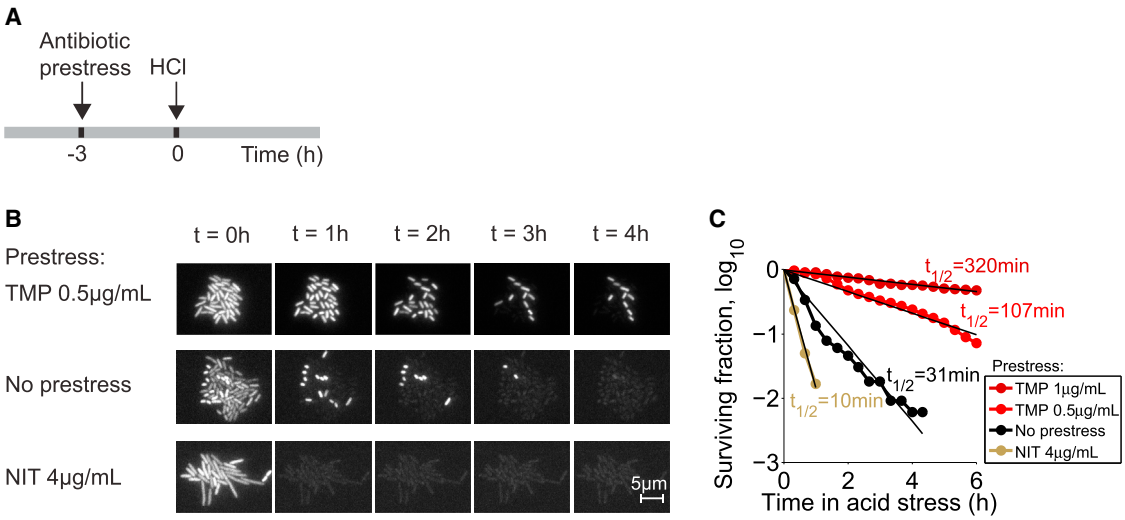

Figure 2. TMP Prestress Cross-Protects Bacteria from Subsequent Acid Challenge

(A) Experimental procedure: bacteria growing in microcolonies in a microfluidics device were prestressed for 3 hr and then subjected to extreme acid stress with HCl at pH 3 (STAR Methods); the antibiotic was removed during the extreme acid stress.

(B) Microscopy images of cells at various time points during the acid stress, with or without 0.5 μg/mL TMP or 4 μg/mL NIT prestress (white is the fluorescent protein used for segmentation). Scale bar, 5 μm.

(C) Fraction of surviving bacteria after addition of HCl and linear fits to the $\log_{10}$ values ($t_{1/2}$ is the half-life) after prestress with 1 μg/mL TMP (dark red, number of analyzed single cells n = 91 from four microcolonies), 0.5 μg/mL TMP (light red, n = 181 from five microcolonies), 4 μg/mL NIT (ocher, n = 60 from three microcolonies) or bacteria without prestress (black, n = 330 from four microcolonies). See also Figure S2.

and amplifies the acid stress response activation, consistent with previous results (Burton et al., 2010), it is not essential for triggering the response to TMP.

Organic Acid Stress Induces Similar Acid Stress Response Pulse as TMP

To confirm the specific activation of the acid stress response by TMP, we compared it with the dynamic response triggered by formic acid. We adjusted the concentration of formic acid to achieve a similar initial growth rate drop as with TMP (Figure S1D). Following this challenge, bacterial growth rate thereafter recovered similarly to the TMP challenge, but to a higher final rate. Under these conditions, formic acid induced a strikingly similar pulse in the same acid stress and RpoS-regulated promoters as TMP (Figure 1E). Expression after this pulse settled back to slightly higher levels than before the stress. These pulse-like dynamics may result from autoregulation and the short half-life of the acid stress regulator GadE (Heuveling et al., 2008; Hommais et al., 2004; Ma et al., 2004) and confirm previous reports (Stincone et al., 2011). Promoters that are related to acid stress but independent of RpoS and GadE, such as the pH-sensitive formate channel *focA* and the alternative sigma factor *rpoE*, had similar dynamics (Figure 1E). Overall, these data show that the dynamic response to an organic acid is similar to the acid stress response induction under the antibiotic TMP.

TMP Cross-Protects Bacteria from Subsequent Acid Stress

We thus hypothesized that the acid stress response induced by TMP could cross-protect bacteria from subsequent acid stress, similar to the effect of a mild acid prestress (Arnold et al., 2001; Leyer and Johnson, 1993; Ryu and Beuchat, 1998). To test this idea, we stressed microcolonies growing in a microfluidics device with TMP and, after 3 hr, switched to medium at pH 3 without antibiotic (Figure 2A; STAR Methods). Under this acid stress, bacteria stopped growing and started lysing within minutes (detected by sudden loss of fluorescence; Lowder et al., 2000; Figure 2B; Movies S1 and S2). The survival curves approximately followed an exponential decay characteristic of a Poisson process for which the probability of cell death remains constant with time (Figure 2C). Cells that had not been prestressed lysed rapidly (half-life 31 ± 2 min); in contrast, cells prestressed with TMP had greatly extended survival (half-lives of 107 ± 6 min and 320 ± 11 min for 0.5 and 1 μg/mL TMP, respectively; Figure 2C). Thus, pre-exposure to TMP strongly protects bacteria from subsequent acid stress. By contrast, pre-treatment with NIT, which downregulates acid stress promoters (Figure 1D), caused individual cells to lyse even faster than in the control (half-life 9.8 ± 0.8 min; Figures 2B and 2C). Taken together, these data show that antibiotics can protect or sensitize bacteria to subsequent acid stress in a way that can be explained by their global transcriptional response.

To test the role of RpoS in acid protection under our conditions, we measured TMP-induced acid protection in an *rpoS* deletion strain (STAR Methods). Consistent with the lower basal levels of *gadBC* in an *rpoS* deletion strain (Figure S1C), this strain was more sensitive to acid without TMP prestress. TMP prestress protected the *rpoS* deletion strain, albeit less than the wild-type (Figures S2A and S2B); this is consistent with the weaker *gadBC* induction in an *rpoS* deletion strain (Figure S1C). Acid stress is known to increase *rpoS* transcription (Hommais et al., 2004) and a drop in intracellular ATP levels, a downstream effect of folate biosynthesis inhibition by TMP (Kwon et al., 2010), can additionally enrich RpoS due to decreased degradation by

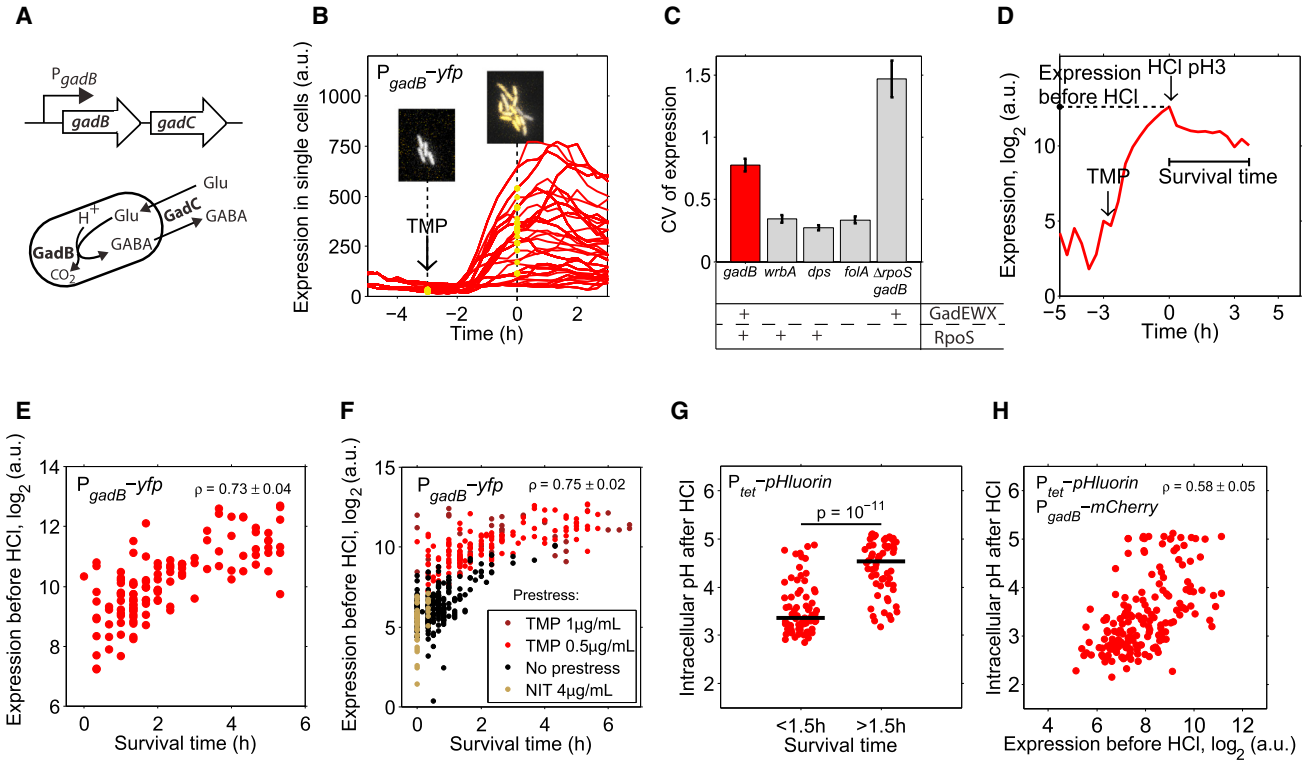

Figure 3. Expression of the Acid Stress Operon *gadBC* Is Highly Variable and Predicts Survival of Single Cells under Acid Stress by Maintaining a Higher Intracellular pH

(A) Schematic of the *gadBC* operon and the function of GadB and GadC. Upon intracellular acidification, GadB catalyzes a proton-consuming reaction on glutamate (Glu) decreasing the intracellular proton concentration in concert with the antiporter GadC that exchanges the product γ-aminobutyric acid (GABA) for glutamate.

(B) Expression of P_{gadB}-*yfp* in response to sudden TMP addition (0.5 μg/mL) at time −3 hr in single cells (n = 26 from two microcolonies). Microscopy images of one microcolony at time points −3 hr and 0 hr are shown; fluorescent protein used for segmentation is gray, yellow fluorescent protein (YFP) is yellow. Yellow dots are *gadBC* expression of cells in the depicted microcolony.

(C) Coefficient of variation (CV) as a measure for cell-to-cell variability in gene expression 3 hr after TMP addition for different promoter-*yfp* constructs (P_{gadB}-*yfp*, P_{wrbA}-*yfp*, P_{dps}-*yfp*, P_{folA}-*yfp*, Δ*rpoS* P_{gadB}-*yfp*). For each promoter, at least 78 cells from at least three microcolonies were analyzed; error bars are from bootstrapping (STAR Methods). Regulation by GadEWX and/or RpoS is shown by "+."

(D) Representative trace of a cell expressing P_{gadB}-*yfp* prestressed with TMP and 3 hr later with HCl at pH 3. Survival time is the time from HCl addition until cell lysis; expression level before HCl was measured as shown.

(E) Expression of P_{gadB}-*yfp* right before HCl addition versus single-cell survival time. Data are from 122 cells in three microcolonies; only cells dying during the time course of the experiment are shown and analyzed. Pearson correlation coefficient is $\rho = 0.73 \pm 0.04$, $p = 3 \times 10^{-21}$.

(F) Same as for (E), but for additional prestressors: 1 μg/mL TMP (n = 44), 4 μg/mL NIT (n = 47), and no prestress (n = 223). For each condition, at least two microcolonies were analyzed. Pearson correlation coefficient for the combined data is $\rho = 0.75 \pm 0.02$, $p = 2 \times 10^{-81}$; error in (E) and (F) is from bootstrapping (STAR Methods). See also Figure S3 for the correlation between the expression from different promoters and survival time.

(G) Intracellular pH of individual cells 10 min after HCl addition, measured with constitutively expressed *pHluorin* (STAR Methods); left: cells that survived <1.5 hr; right: cells that survived >1.5 hr. Medians (black lines) are significantly different ($p = 10^{-11}$, Wilcoxon rank-sum test). Data are from 127 cells in six microcolonies, with no significant differences between the microcolonies. See also Figure S4.

(H) Intracellular pH 10 min after HCl addition versus expression of P_{gadB}-*mCherry* right before HCl addition in single cells (n = 186 from six microcolonies). Spearman correlation coefficient is $\rho = 0.58 \pm 0.05$, $p = 1 \times 10^{-17}$; error from bootstrapping (STAR Methods). Intracellular pH values <3 occur due to large measurement errors and low sensitivity of *pHluorin* at these low pH values (Figure S4B).

the ATP-dependent ClpXP protease (Peterson et al., 2012). These data support that RpoS is not essential for the TMP-induced cross-protection, but it increases the basal level of acid protection, and its induction in response to TMP amplifies the cross-protection.

Expression of the Acid Stress Operon *gadBC* under TMP Is Highly Variable and Predicts Single-Cell Survival

Promoters from the glutamate-dependent acid stress response system were previously found to be highly variable from cell to cell under unstressed conditions (Silander et al., 2012). We therefore wanted to know how variable the expression of this acid stress response was under TMP stress. To this end, we integrated a transcriptional yellow fluorescent protein reporter for the *gadB* promoter (P_{gadB}-*yfp*) into the chromosome (STAR Methods). We selected the *gadB* promoter as it controls the expression of two proteins, GadB and GadC, which act together to lower the intracellular proton concentration (Figure 3A). Using time-lapse microscopy, we observed that the *gadB* promoter was upregulated within 3 hr after TMP addition (Figure 3B),

consistent with our population-level experiments (Figures 1D and 1E); fold-changes varied drastically among cells, ranging from virtually no change to a >30-fold increase. Variability in *gadBC* expression (quantified as coefficient of variation 3 hr after TMP addition) was high compared with the RpoS-regulated promoters *wrbA* and *dps* (Figure 3C), which also showed pulse-like dynamics in their average response (Figure 1E; Table S1). Further, *folA* which codes for dihydrofolate reductase (DHFR, the target of TMP) and is not regulated by acid stress or RpoS, but upregulated under TMP (Keseler et al., 2013), was considerably less variable than *gadBC* (Figure 3C). In addition, this high variability in *gadBC* expression was independent of RpoS, as the coefficient of variation of the expression level in an *rpoS* deletion strain was still extremely high (Figure 3C). In the Δ*rpoS* strain, the basal *gadBC* expression level was lower (Figure S1C), which can explain the even higher noise compared with the wild-type strain (Figure 3C; Taniguchi et al., 2010). These data show that *gadBC* induction in response to TMP is highly variable, consistent with previous results on GadEWX-regulated genes in other conditions (Silander et al., 2012), and that this variability is independent of RpoS.

We reasoned that the highly variable *gadBC* expression in response to TMP might explain the variability in single-cell survival times under subsequent acid stress (Figures 2B and 2C). Indeed, single-cell *gadBC* expression right before the acid stress was strongly correlated with the survival time ($\rho = 0.73$, $p = 3 \times 10^{-21}$; Figures 3D and 3E). A 2-fold increase in *gadBC* expression prolonged survival on average by almost 2 hr. A similar correlation occurred in a control without prestress ($\rho = 0.62$, $p = 3 \times 10^{-25}$; Figure 3F) and when pooling data from different prestresses and no prestress ($\rho = 0.75$, $p = 2 \times 10^{-81}$; Figure 3F). In contrast, *wrbA*, *dps*, or *folA* expression correlated only weakly to moderately with survival, respectively (Figure S3), with the weakest correlation for *folA*, which is neither regulated by RpoS nor GadEWX. Overall, these data show that the specifically noisy *gadBC* expression under TMP predicts single-cell survival upon sudden acid stress, supporting the functional importance of GadB/C in cross-protection and suggesting an important role of these proteins in phenotypically diversifying the bacterial population.

Higher Intracellular pH under HCl Entails Longer Survival Times and Correlates with *gadBC* Expression before HCl

To test whether single-cell survival depends directly on the function of GadB/C, namely the reduction of the intracellular proton concentration, we monitored the intracellular pH using *pHluorin*, a ratiometric GFP variant which was calibrated as described (Figures S4A and S4B; STAR Methods) (Martinez et al., 2012; Miesenböck et al., 1998). When TMP-prestressed cells were exposed to sudden acid stress, their intracellular pH dropped strongly and showed high cell-to-cell variability (>5-fold increase in SD; Figure S4C). The mean pH of cells that survived for at least 10 min was 3.9 ± 0.7, consistent with population-level measurements (Richard and Foster, 2004) and close to the pH optimum of GadB (McCormick and Tunnicliff, 2001; Pennacchietti et al., 2009). The intracellular pH right after HCl addition was significantly higher for cells that survived for longer than 1.5 hr (Figure 3G; $p = 10^{-11}$); no such relation held for the intracellular pH right before the acid stress (Figure S4D). The relation between pH and survival in acid was, however, not perfect (Figure 3G), consistent with previous results that pH is not the sole factor influencing survival (Richard and Foster, 2004); this imperfect relation might also be due to limitations in intracellular pH measurement with *pHluorin* below pH 5 (Martinez et al., 2012; Miesenböck et al., 1998). When switching back to normal growth

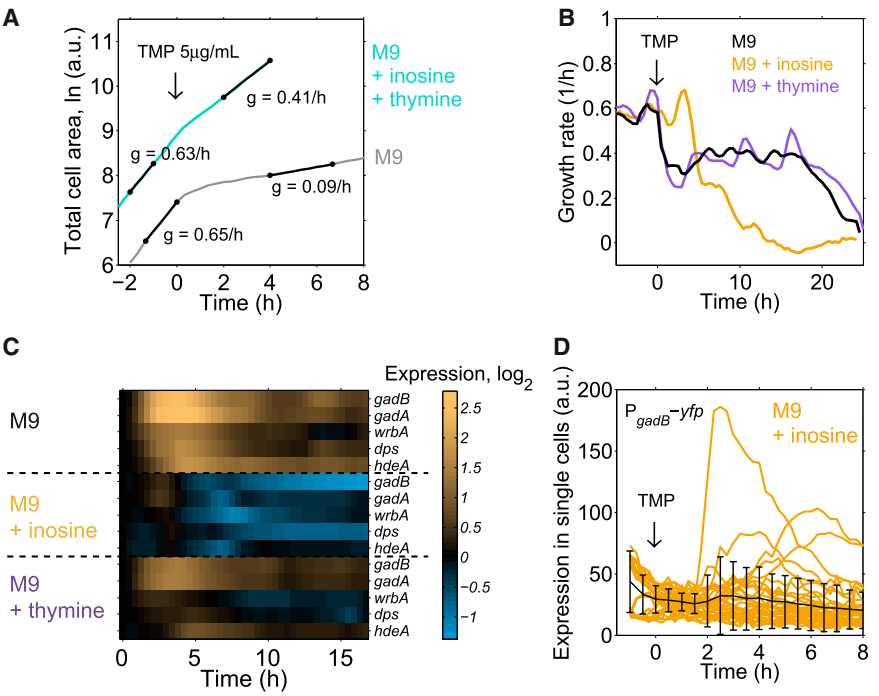

Figure 4. Supplementation with Inosine Bases, but Not with Thymine Bases, Eliminates Acid Stress Response Activation

(A) Total cell area over time and fitted growth rates of one microcolony each in response to high concentrations of TMP (5 μg/mL) in normal M9 medium (gray) and in M9 medium supplemented with inosine and thymine (cyan). Black lines depict regions in which colony growth rate g was fitted.

(B) Growth rate over time in inosine (orange) or thymine (purple) supplemented cultures in response to 0.5 μg/mL TMP, measured with our dilution protocol as in Figure 1.

(C) Expression of acid stress and RpoS promoters (*gadB*, *gadA*, *wrbA*, *dps*, *hdeA*) over time in response to TMP added at time zero as in Figure 1 with inosine and thymine supplemented throughout the experiment, compared with medium without supplements.

(D) Expression from chromosomally integrated P_{gadB}-*yfp* over time in response to 1 μg/mL TMP in inosine supplemented medium is not pulsing in single cells (orange, n = 39 from two microcolonies). Only rarely, individual cells also show an increased expression under these conditions. Black lines are mean and SD of two microcolonies.

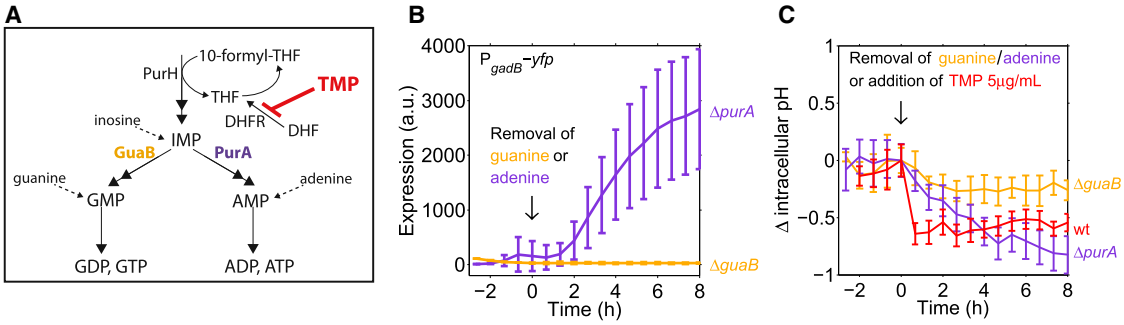

Figure 5. Depletion of Adenine Nucleotides, a Downstream Effect of DHFR Inhibition by TMP, Causes Acid Stress Response Activation and an Intracellular pH Drop

(A) Schematic of the purine biosynthesis pathway. TMP (red) inhibits DHFR (FolA) which catalyzes the production of tetrahydrofolate (THF) from dihydrofolate (DHF). 10-formyltetrahydrofolate (10-formyl-THF), a derivative of THF, is needed for the production of inosine monophosphate (IMP), the precursor for guanine and adenine nucleotides. Inosine, adenine, and guanine can be supplemented and enter the pathway as indicated (dotted arrows).

(B) P_{gadB}-*yfp* expression over time averaged over single cells in *purA* (n = 58 from one microcolony) and *guaB* (n = 8 from one microcolony) deletion mutants in response to sudden removal of adenine or guanine, respectively, mimicking different downstream effects of TMP.

(C) Change in intracellular pH in Δ*purA* (n = 53 from one microcolony) and Δ*guaB* (n = 7 from one microcolony) mutants in response to sudden removal of adenine or guanine, respectively, and in the wild-type without supplements treated with 5 μg/mL TMP (red, n = 14 from one microcolony). Lines in (B) and (C) are means, errors bars are SDs for a microcolony. See also Figure S5.

medium, some surviving bacteria resumed growth during the time course of the experiment (Movie S2) while others did not resume growth or lysed. In contrast, cells classified as dead based on their loss of fluorescence during the acid stress never resumed growth.

To test whether higher intracellular pH after HCl addition is caused by high *gadBC* expression levels before the HCl stress, we measured P_{gadB}-*mCherry* expression and intracellular pH in the same cell. Even though *mCherry* has a longer maturation time which impedes dynamic measurements (STAR Methods), we still detected a strong correlation ($\rho = 0.58$, $p = 1 \times 10^{-17}$; Figure 3H). Together with the correlation between *gadBC* expression and survival, these results directly connect the function of the acid stress proteins GadB/C to survival: higher *gadBC* expression enables cells to maintain higher intracellular pH under severe acid stress, which in turn prolongs survival.

Depletion of Adenine Bases under TMP Leads to a pH Drop and Activation of the Acid Stress Response

Which molecular pathways and physiological changes lead to the activation of acid stress promoters in response to TMP? The main downstream effects of dihydrofolate reductase (DHFR or FolA) inhibition are the depletion of amino acids, purine bases, and thymine (Amyes and Smith, 1974; Kwon et al., 2010). We first confirmed that DHFR inhibition by TMP in our conditions could be rescued by supplementing purine bases and thymine: we observed only minor growth rate changes in response to even high concentrations of TMP when inosine (a purine base) and thymine were added to the growth medium (Figure 4A). Next, to distinguish whether thymine or purine depletion induced the acid stress response, we supplemented either component separately to the growth medium: thymine had little effect, but when inosine was supplemented, acid stress promoters were no longer upregulated (Figures 4C and 4D). Under these conditions, also the growth rate response to TMP changed drastically (Figure 4B) in that growth was unaffected for ~4 hr, but completely halted afterward. With supplemented inosine, TMP is bactericidal and leads to "thymineless death": in contrast to purine depletion, which results in growth arrest, bacteria cannot sense the depletion of thymine bases and incur severe DNA damage (Amyes and Smith, 1974; Kwon et al., 2010). We thus hypothesized that the acid stress response to TMP is activated as a downstream effect of the depletion of purine bases.

To further pinpoint whether guanine nucleotide depletion or adenine nucleotide depletion cause the acid stress response induction, we mimicked the inhibitory effect of TMP on each of these biosynthesis pathways separately. Specifically, we measured *gadBC* expression under sudden guanine and adenine nucleotide depletion, respectively, using the deletion mutants *ΔguaB* and *ΔpurA* (Baba et al., 2006). Both enzymes are downstream of the reaction catalyzed by PurH which consumes 10-formyltetrahydrofolate (Figure 5A): GuaB is the first enzyme in the synthesis of guanine nucleotides from inosine monophosphate (IMP) and PurA catalyzes the first step in the synthesis of adenine nucleotides from IMP. We grew these mutants in medium supplemented with their respective purine base (guanine for *ΔguaB* and adenine for *ΔpurA*) and induced depletion by sudden removal of these purine bases in the microfluidics device (STAR Methods). In both cases, growth rates dropped (Figure S5A), presumably due to the complete depletion of purine bases. While *gadBC* expression stayed low and showed virtually no response to sudden guanine removal, it strongly increased upon adenine depletion (Figure 5B).

To test whether acidification of the cytoplasm causes acid stress induction, we measured the intracellular pH in the deletion mutants after adenine or guanine removal and in the wild-type under TMP stress. The intracellular pH clearly dropped in the *ΔpurA* assay, while virtually no change in pH occurred in the *ΔguaB* assay (Figure 5C). We also observed an immediate drop in intracellular pH by ~0.65 pH units in response to high concentrations of TMP (Figure 5C); a similar but weaker pH drop also occurred in response to lower TMP concentrations (Figure S5B). The pH dynamics following TMP addition were different from those upon adenine removal in the Δ*purA* mutant,

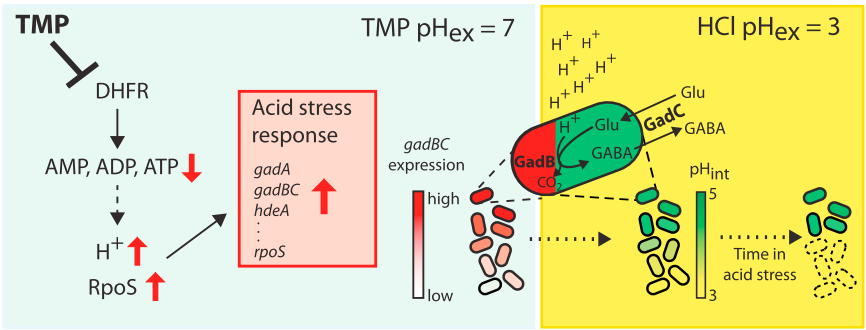

Figure 6. Summary of the Molecular Mechanisms by Which TMP Cross-Protects from Acid Stress

See main text for details; every single cell has its distinct *gadBC* level (red) which influences its intracellular pH (green). DHFR, dihydrofolate reductase; AMP, ADP, ATP, adenine nucleotides; RpoS, general stress sigma factor; H^+, proton; *gadA*, *gadBC*, *hdeA*, acid stress promoters; *rpoS*, RpoS promoter; Glu, glutamate; GABA, γ-aminobutyric acid; pH_{int}, intracellular pH; pH_{ex}, extracellular pH.

possibly due to the different point of inhibition in the adenine biosynthesis pathway and different dynamics of adenine nucleotide depletion. While ATP and adenosine were suggested to have a protective role in acid resistance (Sun et al., 2011, 2012), the molecular mechanisms that cause this intracellular acidification upon adenine depletion remain to be further elucidated.

Deletion of the NADH Dehydrogenase Amplifies pH Drop, *gadBC* Response, and Growth Rate Drop under TMP

To further validate the contribution of the intracellular pH drop to acid stress response induction under TMP, we screened 160 gene deletion mutants (Baba et al., 2006) for changes in growth rate and *gadBC* expression. Mutants were selected to cover genes involved in acid stress response activation and pH homeostasis (STAR Methods). The deletion strains Δ*gadE* and Δ*rcsB* no longer upregulated *gadBC* expression (Figure S6A), consistent with the role of these genes as important regulators of the glutamate-dependent acid resistance system (Foster, 2004; Krin et al., 2010). Like most mutants screened, Δ*gadE* and Δ*rcsB* had only minor fitness disadvantages under TMP, suggesting that the glutamate-dependent acid stress response is dispensable under the applied TMP concentrations (Figure S6B). Interestingly, the Δ*nuoC* strain showed an aggravated growth rate drop (Figure S6B) and prolonged and amplified *gadBC* expression (Figure S6A) and pH drop (Figure S6C). NuoC is an essential component for the proper formation of the proton-pumping NADH dehydrogenase I complex (Sinha et al., 2015), which can likely protect from mild acid stress (Kanjee and Houry, 2013; Krulwich et al., 2011). Other respiratory chain mutants did not show a strongly altered response. Thus, amplifying the pH drop via reduced proton pumping in the Δ*nuoC* strain results in an amplified and prolonged acid stress response, further supporting that an intracellular pH drop is a key trigger of the acid stress response to TMP.

DISCUSSION

We showed that the antibiotic TMP induces a functional acid stress response. This happens via the depletion of adenine nucleotides, which leads to an intracellular pH drop and RpoS induction (Figure 6). This acid stress response, including the acid resistance proteins GadB and GadC, cross-protects bacteria from subsequent acid stress. Single-cell survival under acid stress is predictable from the variable expression of *gadBC*, with a higher intracellular pH in cells that survive longer (Figure 6). In summary, our results revealed the chain of events and molecular mechanisms by which the antibiotic TMP cross-protects from an environmental acid stress. How the depletion of adenine nucleotides leads to intracellular acidification and acid stress induction is not clear yet. We speculate that decreased intracellular ATP levels either impair pH homeostasis or induce other ATP-generating, acidifying mechanisms.

Most antibiotics affect the expression of many bacterial genes, with consequences for microbial communities and host-microbe interactions (Hoffman et al., 2005; Justice et al., 2008; Maurice et al., 2013). Some of these regulatory responses are direct downstream effects of drug target inhibition but the cause and functional role of most gene expression changes is rather obscure (Price et al., 2013). Here, precise measurements of the genome-wide transcriptional response dynamics to antibiotics empowered us to identify a specific stressor (acid) against which TMP could cross-protect. This approach is generally applicable and will enable the systematic identification of pairs of environmental stressors and cross-protecting or -sensitizing antibiotics, together with the optimal time-window that maximizes these effects. Based on our data (Figure 1D), we expect specific cross-protection effects between TET or NIT and oxidative stress, and NIT and DNA damaging agents. The RpoS induction under TMP might further cross-protect from various environmental stressors. More generally, our results suggest that the gene expression state induced by an antibiotic can completely change the cell's fitness in a subsequent environment. This finding may lead to new strategies for designing advanced treatments that potentiate the effects of antibiotics (Allison et al., 2011; Morones-Ramirez et al., 2013) and exploit bacterial vulnerabilities by temporally switching between different antibiotics in ways that accelerate the eradication of pathogens.

By focusing on the *gadB* promoter, which controls acid resistance proteins that are well characterized at the population level, we were able to predict and functionally explain single-cell survival and its high variability among cells. Our single-cell study thus exploited natural variability to infer causal chains of molecular events from temporal correlations. This approach can further suggest survival strategies: the high variability in *gadBC* expression observed here may hint at a bet-hedging strategy in which populations can maximize their fitness by keeping a fraction of cells in a less-fit state that prepares them for a future environment. The best-known example for this kind of

bet-hedging strategy is bacterial persistence (Balaban et al., 2004). It remains to be tested if a bet-hedging strategy underlies the response characteristics of the glutamate-dependent acid resistance system revealed here.

Overall, this work shows how exposure to antibiotics triggers bacterial responses that can subsequently alter cell physiology and directly affect fitness upon a change in environment. Such environmental changes are common in an infected host where bacteria often encounter antibiotics together with environmental stressors such as acid, reactive oxygen species, or heat. In particular, immune cells attack bacteria with oxidative bursts in an acidic phagosome (Audia et al., 2001). Cross-protection effects may therefore complicate antimicrobial treatment by impeding the eradication of bacteria that were exposed to antibiotics. An acidic environment can also be found in the mammalian digestive system, and can be caused by gastric acid, food, other drugs, or other bacterial species; here, the changed sensitivity of a particular species to acid may have effects on microbiome composition. Future research will show how widespread cross-protection and -sensitivity between antibiotics and environmental stressors are, and how they can be prevented or exploited in treatments.

STAR★METHODS

Detailed methods are provided in the online version of this paper and include the following:

- KEY RESOURCES TABLE
- CONTACT FOR REAGENT AND RESOURCE SHARING
- EXPERIMENTAL MODEL AND SUBJECT DETAILS
  - Strains, Antibiotics, and Culture Conditions
- METHOD DETAILS
  - Gene Expression Measurements with Robotic System
  - Plasmid Construction
  - Strain Construction and Verification
  - Microfluidics and Time-Lapse Microscopy
  - Measurements of Intracellular pH
- QUANTIFICATION AND STATISTICAL ANALYSIS
  - Analysis of the Population-Level Data
  - Analysis of Single-Cell Data

SUPPLEMENTAL INFORMATION

Supplemental Information includes six figures, three tables, and two movies and can be found with this article online at http://dx.doi.org/10.1016/j.cels.2017.03.001.

AUTHOR CONTRIBUTIONS

K.M. and T.B conceived the study and designed the experiments. K.M. performed the experiments and analyzed the data. G.R. designed and G.R. and K.M. constructed chromosomal integration strains. K.M., G.R., and T.B. wrote the manuscript.

ACKNOWLEDGMENTS

We thank Fabienne Jesse, Anna Andersson, Martin Lukačišin, Gašper Tkačik, James Locke, Nassos Typas, Joan Slonczewski, and Peter Lund for critical comments on the manuscript, and Uwe Sauer, Teuta Pilizota, Călin Guet, Terry Hwa, and the whole Bollenbach group for fruitful discussions. We further thank Joan Slonczewski, the Court lab, and Tobias Bergmiller for sharing plasmids.

This work was supported in part by Marie Curie Career Integration Grant (CIG) no. 303507, Austrian Science Fund (FWF) standalone grant P 27201-B22, and HFSP program grant no. RGP0042/2013.

Received: September 6, 2016
Revised: December 14, 2016
Accepted: March 1, 2017
Published: March 22, 2017

REFERENCES

Allison, K.R., Brynildsen, M.P., and Collins, J.J. (2011). Metabolite-enabled eradication of bacterial persisters by aminoglycosides. Nature *473*, 216–220.

Al-Nabulsi, A.A., Osaili, T.M., Shaker, R.R., Olaimat, A.N., Jaradat, Z.W., Zain Elabedeen, N.A., and Holley, R.A. (2015). Effects of osmotic pressure, acid, or cold stresses on antibiotic susceptibility of *Listeria monocytogenes*. Food Microbiol. *46*, 154–160.

Amyes, S.G.B., and Smith, J.T. (1974). Trimethoprim action and its analogy with thymine starvation. Antimicrob. Agents Chemother. *5*, 169–178.

Andersson, D.I., and Hughes, D. (2014). Microbiological effects of sublethal levels of antibiotics. Nat. Rev. Microbiol. *12*, 465–478.

Arnold, C.N., McElhanon, J., Lee, A., Leonhart, R., and Siegele, D.A. (2001). Global analysis of *Escherichia coli* gene expression during the acetate-induced acid tolerance response. J. Bacteriol. *183*, 2178–2186.

Arnoldini, M., Vizcarra, I.A., Peña-Miller, R., Stocker, N., Diard, M., Vogel, V., Beardmore, R.E., Hardt, W.-D., and Ackermann, M. (2014). Bistable expression of virulence genes in *Salmonella* leads to the formation of an antibiotic-tolerant subpopulation. PLoS Biol. *12*, e1001928.

Audia, J.P., Webb, C.C., and Foster, J.W. (2001). Breaking through the acid barrier: an orchestrated response to proton stress by enteric bacteria. Int. J. Med. Microbiol. *291*, 97–106.

Baba, T., Ara, T., Hasegawa, M., Takai, Y., Okumura, Y., Baba, M., Datsenko, K.A., Tomita, M., Wanner, B.L., and Mori, H. (2006). Construction of *Escherichia coli* K-12 in-frame, single-gene knockout mutants: the Keio collection. Mol. Syst. Biol. *2*, 2006.0008.

Balaban, N.Q., Merrin, J., Chait, R., Kowalik, L., and Leibler, S. (2004). Bacterial persistence as a phenotypic switch. Science *305*, 1622–1625.

Basan, M., Zhu, M., Dai, X., Warren, M., Sévin, D., Wang, Y.-P., and Hwa, T. (2015). Inflating bacterial cells by increased protein synthesis. Mol. Syst. Biol. *11*, 836.

Battesti, A., Majdalani, N., and Gottesman, S. (2011). The RpoS-mediated general stress response in *Escherichia coli*. Annu. Rev. Microbiol. *65*, 189–213.

Begley, M., Gahan, C.G.M., and Hill, C. (2002). Bile stress response in *Listeria monocytogenes* LO28: adaptation, cross-protection, and identification of genetic loci involved in bile resistance. Appl. Environ. Microbiol. *68*, 6005–6012.

Belenky, P., Ye, J.D., Porter, C.B.M., Cohen, N.R., Lobritz, M.A., Ferrante, T., Jain, S., Korry, B.J., Schwarz, E.G., Walker, G.C., et al. (2015). Bactericidal antibiotics induce toxic metabolic perturbations that lead to cellular damage. Cell Rep. *13*, 968–980.

Berry, D.B., and Gasch, A.P. (2008). Stress-activated genomic expression changes serve a preparative role for impending stress in yeast. Mol. Biol. Cell *19*, 4580–4587.

Bollenbach, T., Quan, S., Chait, R., and Kishony, R. (2009). Nonoptimal microbial response to antibiotics underlies suppressive drug interactions. Cell *139*, 707–718.

Brazas, M.D., and Hancock, R.E.W. (2005). Using microarray gene signatures to elucidate mechanisms of antibiotic action and resistance. Drug Discov. Today *10*, 1245–1252.

Bryant, D.W., and McCalla, D.R. (1980). Nitrofuran induced mutagenesis and error prone repair in *Escherichia coli*. Chem. Biol. Interact. *31*, 151–166.

Burton, N.A., Johnson, M.D., Antczak, P., Robinson, A., and Lund, P.A. (2010). Novel aspects of the acid response network of *E. coli* K-12 are revealed by a study of transcriptional dynamics. J. Mol. Biol. *401*, 726–742.

Castanie-Cornet, M.-P., Penfound, T.A., Smith, D., Elliott, J.F., and Foster, J.W. (1999). Control of acid resistance in *Escherichia coli*. J. Bacteriol. *181*, 3525–3535.

Cherepanov, P.P., and Wackernagel, W. (1995). Gene disruption in *Escherichia coli*: TcR and KmR cassettes with the option of Flp-catalyzed excision of the antibiotic-resistance determinant. Gene *158*, 9–14.

Cox, R.S., Dunlop, M.J., and Elowitz, M.B. (2010). A synthetic three-color scaffold for monitoring genetic regulation and noise. J. Biol. Eng. *4*, 10.

Datsenko, K.A., and Wanner, B.L. (2000). One-step inactivation of chromosomal genes in *Escherichia coli* K-12 using PCR products. Proc. Natl. Acad. Sci. USA *97*, 6640–6645.

Datta, S., Costantino, N., and Court, D.L. (2006). A set of recombineering plasmids for gram-negative bacteria. Gene *379*, 109–115.

De Biase, D., Tramonti, A., Bossa, F., and Visca, P. (1999). The response to stationary-phase stress conditions in *Escherichia coli*: role and regulation of the glutamic acid decarboxylase system. Mol. Microbiol. *32*, 1198–1211.

El Meouche, I., Siu, Y., and Dunlop, M.J. (2016). Stochastic expression of a multiple antibiotic resistance activator confers transient resistance in single cells. Sci. Rep. *6*, 19538.

Foster, J.W. (2004). *Escherichia coli* acid resistance: tales of an amateur acidophile. Nat. Rev. Microbiol. *2*, 898–907.

Gama-Castro, S., Salgado, H., Peralta-Gil, M., Santos-Zavaleta, A., Muñiz-Rascado, L., Solano-Lira, H., Jimenez-Jacinto, V., Weiss, V., García-Sotelo, J.S., López-Fuentes, A., et al. (2011). RegulonDB version 7.0: transcriptional regulation of *Escherichia coli* K-12 integrated within genetic sensory response units (Gensor Units). Nucleic Acids Res. *39*, D98–D105.

Goh, E.B., Yim, G., Tsui, W., McClure, J., Surette, M.G., and Davies, J. (2002). Transcriptional modulation of bacterial gene expression by subinhibitory concentrations of antibiotics. Proc. Natl. Acad. Sci. USA *99*, 17025–17030.

Goodson, M., and Rowbury, R.J. (1989). Habituation to normally lethal acidity by prior growth of *Escherichia coli* at a sub-lethal acid pH value. Lett. Appl. Microbiol. *8*, 77–79.

Hersh, B.M., Farooq, F.T., Barstad, D.N., Blankenhorn, D.L., and Slonczewski, J.L. (1996). A glutamate-dependent acid resistance gene in *Escherichia coli*. J. Bacteriol. *178*, 3978–3981.

Heuveling, J., Possling, A., and Hengge, R. (2008). A role for Lon protease in the control of the acid resistance genes of *Escherichia coli*. Mol. Microbiol. *69*, 534–547.

Hoffman, L.R., D'Argenio, D.A., MacCoss, M.J., Zhang, Z., Jones, R.A., and Miller, S.I. (2005). Aminoglycoside antibiotics induce bacterial biofilm formation. Nature *436*, 1171–1175.

Hommais, F., Krin, E., Coppée, J.-Y., Lacroix, C., Yeramian, E., Danchin, A., and Bertin, P. (2004). GadE (YhiE): a novel activator involved in the response to acid environment in *Escherichia coli*. Microbiology *150*, 61–72.

Jenkins, D.E., Schultz, J.E., and Matin, A. (1988). Starvation-induced cross protection against heat or H2O2 challenge in *Escherichia coli*. J. Bacteriol. *170*, 3910–3914.

Justice, S.S., Hunstad, D.A., Cegelski, L., and Hultgren, S.J. (2008). Morphological plasticity as a bacterial survival strategy. Nat. Rev. Microbiol. *6*, 162–168.

Kanjee, U., and Houry, W.A. (2013). Mechanisms of acid resistance in *Escherichia coli*. Annu. Rev. Microbiol. *67*, 65–81.

Keseler, I.M., Mackie, A., Peralta-Gil, M., Santos-Zavaleta, A., Gama-Castro, S., Bonavides-Martínez, C., Fulcher, C., Huerta, A.M., Kothari, A., Krummenacker, M., et al. (2013). EcoCyc: fusing model organism databases with systems biology. Nucleic Acids Res. *41*, D605–D612.

Krin, E., Danchin, A., and Soutourina, O. (2010). RcsB plays a central role in H-NS-dependent regulation of motility and acid stress resistance in *Escherichia coli*. Res. Microbiol. *161*, 363–371.

Krulwich, T.A., Sachs, G., and Padan, E. (2011). Molecular aspects of bacterial pH sensing and homeostasis. Nat. Rev. Microbiol. *9*, 330–343.

Kwon, Y.K., Higgins, M.B., and Rabinowitz, J.D. (2010). Antifolate-induced depletion of intracellular glycine and purines inhibits thymineless death in *E. coli*. ACS Chem. Biol. *5*, 787–795.

Lennox, E.S. (1955). Transduction of linked genetic characters of the host by bacteriophage P1. Virology *1*, 190–206.

Lewin, C.S., and Amyes, S.G.B. (1991). The role of the SOS response in bacteria exposed to zidovudine or trimethoprim. J. Med. Microbiol. *34*, 329–332.

Leyer, G.J., and Johnson, E.A. (1993). Acid adaptation induces cross-protection against environmental stresses in *Salmonella typhimurium*. Appl. Environ. Microbiol. *59*, 1842–1847.

Lin, J., Smith, M.P., Chapin, K.C., Baik, H.S., Bennett, G.N., and Foster, J.W. (1996). Mechanisms of acid resistance in enterohemorrhagic *Escherichia coli*. Appl. Environ. Microbiol. *62*, 3094–3100.

Locke, J.C.W., Young, J.W., Fontes, M., Jiménez, M.J.H., and Elowitz, M.B. (2011). Stochastic pulse regulation in bacterial stress response. Science *334*, 366–369.

Lowder, M., Unge, A., Maraha, N., Jansson, J.K., Swiggett, J., and Oliver, J.D. (2000). Effect of starvation and the viable-but-nonculturable state on green fluorescent protein (GFP) fluorescence in GFP-tagged *Pseudomonas fluorescens* A506. Appl. Environ. Microbiol. *66*, 3160–3165.

Lutz, R., and Bujard, H. (1997). Independent and tight regulation of transcriptional units in *Escherichia coli* via the LacR/O, the TetR/O and AraC/I1-I2 regulatory elements. Nucleic Acids Res. *25*, 1203–1210.

Ma, Z., Masuda, N., and Foster, J.W. (2004). Characterization of EvgAS-YdeO-GadE branched regulatory circuit governing glutamate-dependent acid resistance in *Escherichia coli*. J. Bacteriol. *186*, 7378–7389.

Martín, J.F., and Liras, P. (1989). Organization and expression of genes involved in the biosynthesis of antibiotics and other secondary metabolites. Annu. Rev. Microbiol. *43*, 173–206.

Martinez, K.A., Kitko, R.D., Mershon, J.P., Adcox, H.E., Malek, K.A., Berkmen, M.B., and Slonczewski, J.L. (2012). Cytoplasmic pH response to acid stress in individual cells of *Escherichia coli* and *Bacillus subtilis* observed by fluorescence ratio imaging microscopy. Appl. Environ. Microbiol. *78*, 3706–3714.

Maurice, C.F., Haiser, H.J., and Turnbaugh, P.J. (2013). Xenobiotics shape the physiology and gene expression of the active human gut microbiome. Cell *152*, 39–50.

McCormick, S.J., and Tunnicliff, G. (2001). Kinetics of inactivation of glutamate decarboxylase by cysteine-specific reagents. Acta Biochim. Pol. *48*, 573–578.

McMahon, M.A.S., Xu, J., Moore, J.E., Blair, I.S., and McDowell, D.A. (2007). Environmental stress and antibiotic resistance in food-related pathogens. Appl. Environ. Microbiol. *73*, 211–217.

Megerle, J.A., Fritz, G., Gerland, U., Jung, K., and Rädler, J.O. (2008). Timing and dynamics of single cell gene expression in the arabinose utilization system. Biophys. J. *95*, 2103–2115.

Miesenböck, G., De Angelis, D.A., and Rothman, J.E. (1998). Visualizing secretion and synaptic transmission with pH-sensitive green fluorescent proteins. Nature *394*, 192–195.

Mitchell, A., Romano, G.H., Groisman, B., Yona, A., Dekel, E., Kupiec, M., Dahan, O., and Pilpel, Y. (2009). Adaptive prediction of environmental changes by microorganisms. Nature *460*, 220–224.

Morones-Ramirez, J.R., Winkler, J.A., Spina, C.S., and Collins, J.J. (2013). Silver enhances antibiotic activity against gram-negative bacteria. Sci. Transl. Med. *5*, 190ra81.

Newman, J.R.S., Ghaemmaghami, S., Ihmels, J., Breslow, D.K., Noble, M., DeRisi, J.L., and Weissman, J.S. (2006). Single-cell proteomic analysis of *S. cerevisiae* reveals the architecture of biological noise. Nature *441*, 840–846.

Ni, M., Decrulle, A.L., Fontaine, F., Demarez, A., Taddei, F., and Lindner, A.B. (2012). Pre-disposition and epigenetics govern variation in bacterial survival upon stress. PLoS Genet. *8*, e1003148.

Pennacchietti, E., Lammens, T.M., Capitani, G., Franssen, M.C.R., John, R.A., Bossa, F., and De Biase, D. (2009). Mutation of His465 alters the pH-dependent spectroscopic properties of *Escherichia coli* glutamate decarboxylase and broadens the range of its activity toward more alkaline pH. J. Biol. Chem. *284*, 31587–31596.

Peterson, C.N., Levchenko, I., Rabinowitz, J.D., Baker, T.A., and Silhavy, T.J. (2012). RpoS proteolysis is controlled directly by ATP levels in *Escherichia coli*. Genes Dev. *26*, 548–553.

Price, M.N., Deutschbauer, A.M., Skerker, J.M., Wetmore, K.M., Ruths, T., Mar, J.S., Kuehl, J.V., Shao, W., and Arkin, A.P. (2013). Indirect and suboptimal control of gene expression is widespread in bacteria. Mol. Syst. Biol. *9*, 660.

Qiang, Z., and Adams, C. (2004). Potentiometric determination of acid dissociation constants (pKa) for human and veterinary antibiotics. Water Res. *38*, 2874–2890.

Richard, H., and Foster, J.W. (2004). *Escherichia coli* glutamate- and arginine-dependent acid resistance systems increase internal pH and reverse transmembrane potential. J. Bacteriol. *186*, 6032–6041.

Ryu, J.-H., and Beuchat, L.R. (1998). Influence of acid tolerance responses on survival, growth, and thermal cross-protection of *Escherichia coli* O157:H7 in acidified media and fruit juices. Int. J. Food Microbiol. *45*, 185–193.

Sánchez-Romero, M.A., and Casadesús, J. (2014). Contribution of phenotypic heterogeneity to adaptive antibiotic resistance. Proc. Natl. Acad. Sci. USA *111*, 355–360.

Sangurdekar, D.P., Zhang, Z., and Khodursky, A.B. (2011). The association of DNA damage response and nucleotide level modulation with the antibacterial mechanism of the anti-folate drug Trimethoprim. BMC Genomics *12*, 583.

Seo, S.W., Kim, D., O'Brien, E.J., Szubin, R., and Palsson, B.O. (2015). Decoding genome-wide GadEWX-transcriptional regulatory networks reveals multifaceted cellular responses to acid stress in *Escherichia coli*. Nat. Commun. *6*, 7970.

Silander, O.K., Nikolic, N., Zaslaver, A., Bren, A., Kikoin, I., Alon, U., and Ackermann, M. (2012). A genome-wide analysis of promoter-mediated phenotypic noise in *Escherichia coli*. PLoS Genet. *8*, e1002443.

Sinha, P.K., Castro-Guerrero, N., Patki, G., Sato, M., Torres-Bacete, J., Sinha, S., Miyoshi, H., Matsuno-Yagi, A., and Yagi, T. (2015). Conserved amino acid residues of the NuoD segment important for structure and function of *Escherichia coli* NDH-1 (Complex I). Biochemistry (Mosc) *54*, 753–764.

Stincone, A., Daudi, N., Rahman, A.S., Antczak, P., Henderson, I., Cole, J., Johnson, M.D., Lund, P., and Falciani, F. (2011). A systems biology approach sheds new light on *Escherichia coli* acid resistance. Nucleic Acids Res. *39*, 7512–7528.

Sun, Y., Fukamachi, T., Saito, H., and Kobayashi, H. (2011). ATP requirement for acidic resistance in *Escherichia coli*. J. Bacteriol. *193*, 3072–3077.

Sun, Y., Fukamachi, T., Saito, H., and Kobayashi, H. (2012). Adenosine deamination increases the survival under acidic conditions in *Escherichia coli*. J. Appl. Microbiol. *112*, 775–781.

Tagkopoulos, I., Liu, Y.-C., and Tavazoie, S. (2008). Predictive behavior within microbial genetic networks. Science *320*, 1313–1317.

Taniguchi, Y., Choi, P.J., Li, G.W., Chen, H., Babu, M., Hearn, J., Emili, A., and Xie, X.S. (2010). Quantifying *E. coli* proteome and transcriptome with single-molecule sensitivity in single cells. Science *329*, 533–538.

Tsai, M.-F., McCarthy, P., and Miller, C. (2013). Substrate selectivity in glutamate-dependent acid resistance in enteric bacteria. Proc. Natl. Acad. Sci. USA *110*, 5898–5902.

Waksman, S.A. (1961). The role of antibiotics in nature. Perspect. Biol. Med. *4*, 271–287.

Wang, G., and Doyle, M.P. (1998). Heat shock response enhances acid tolerance of *Escherichia coli* O157:H7. Lett. Appl. Microbiol. *26*, 31–34.

Weber, H., Polen, T., Heuveling, J., Wendisch, V.F., and Hengge, R. (2005). Genome-wide analysis of the general stress response network in *Escherichia coli*: σS-dependent genes, promoters, and sigma factor selectivity. J. Bacteriol. *187*, 1591–1603.

Weinstein, D.H., deRijke, S., Chow, C.C., Foruraghi, L., Zhao, X., Wright, E.C., Whatley, M., Maass-Moreno, R., Chen, C.C., and Wank, S.A. (2013). A new method for determining gastric acid output using a wireless pH-sensing capsule. Aliment. Pharmacol. Ther. *37*, 1198–1209.

Young, J.W., Locke, J.C.W., Altinok, A., Rosenfeld, N., Bacarian, T., Swain, P.S., Mjolsness, E., and Elowitz, M.B. (2012). Measuring single-cell gene expression dynamics in bacteria using fluorescence time-lapse microscopy. Nat. Protoc. *7*, 80–88.

Zaslaver, A., Bren, A., Ronen, M., Itzkovitz, S., Kikoin, I., Shavit, S., Liebermeister, W., Surette, M.G., and Alon, U. (2006). A comprehensive library of fluorescent transcriptional reporters for *Escherichia coli*. Nat. Methods *3*, 623–628.

STAR★METHODS

KEY RESOURCES TABLE

REAGENT or RESOURCE	SOURCE	IDENTIFIER
Bacterial and Virus Strains		
Escherichia coli MG1655	Uri Alon lab	N/A
Escherichia coli BW25113	Keio collection (Baba et al., 2006)	https://shigen.nig.ac.jp/ecoli/strain/
MG1655 Δ*intS*::P_{gadB}-*yfp*	This paper, with P_{gadB} amplified from the chromosome	N/A
MG1655 Δ*intS*::P_{wrbA}-*yfp*	This paper, based on P_{wrbA}-*gfp* plasmid from (Zaslaver et al., 2006)	N/A
MG1655 Δ*intS*::P_{dps}-*yfp*	This paper, based on P_{dps}-*gfp* plasmid from (Zaslaver et al., 2006)	N/A
MG1655 Δ*intS*::P_{folA}-*yfp*	This paper, based on P_{folA}-*gfp* plasmid from (Zaslaver et al., 2006)	N/A
BW25113 single gene deletion strains	Keio collection (Baba et al., 2006)	https://shigen.nig.ac.jp/ecoli/strain/
BW25113 Δ*guaB* Δ*intS*::P_{gadB}-*yfp*	This paper, based on strain from the KEIO collection (Baba et al., 2006) and Δ*intS*::P_{gadB}-*yfp*	N/A
BW25113 Δ*purA* Δ*intS*::P_{gadB}-*yfp*	This paper, based on strain from the KEIO collection (Baba et al., 2006) and MG1655 Δ*intS*::P_{gadB}-*yfp*	N/A
MG1655 Δ*intS*::P_{gadB}-*mCherry*	This paper, based on P_{gadB}-*gfp* plasmid and *mCherry* from the plasmid pZS2-123 (Cox et al., 2010)	N/A
MG1655 Δ*rpoS* Δ*intS*::P_{gadB}-*yfp*	This paper, Δ*rpoS* mutation was P1 transduced from the KEIO strain (Baba et al., 2006) and Δ*intS*::P_{gadB}-*yfp* insertion from the strain MG1655 Δ*intS*::P_{gadB}-*yfp*	N/A
Chemicals, Peptides, and Recombinant Proteins		
Trimethoprim	Sigma-Aldrich	92131
Tetracycline hydrate	Sigma-Aldrich	268054
Nitrofurantoin	Sigma-Aldrich	N7878
Chloramphenicol	Sigma-Aldrich	C0378
Kanamycin sulfate	Sigma-Aldrich	K4000
Ampicillin sodium salt	Sigma-Aldrich	A9518
Spectinomycin sulfate	Sigma-Aldrich	PHR1441
Critical Commercial Assays		
CellASIC ONIX microfluidics system	Merck Millipore	N/A
Oligonucleotides		
See Table S3.	This paper	N/A
Recombinant DNA		
Plasmid-based promoter-GFP library	Uri Alon lab (Zaslaver et al., 2006)	N/A
Plasmid pZS11-*pHluorin*	This paper, based on plasmids from (Lutz and Bujard, 1997) and (Martinez et al., 2012)	N/A
Plasmid pZS41-*mCherry*	This paper, based on plasmids from (Lutz and Bujard, 1997) and (Cox et al., 2010)	N/A
Plasmid pUA139 P_{gadB}-*gfp* Amp^R	This paper, based on pUA139 plasmid from (Zaslaver et al., 2006) and P_{gadB} amplified from the chromosome	N/A
Plasmid pSIM19	Donald Court lab (Datta et al., 2006)	https://redrecombineering.ncifcrf.gov/strains–plasmids.html
Plasmid pCP20	(Cherepanov and Wackernagel, 1995)	N/A
Software and Algorithms		
MATLAB version R2011b	MathWorks	N/A
Schnitzcells MATLAB package	(Young et al., 2012)	http://easerver.caltech.edu/wordpress/schnitzcells/

CONTACT FOR REAGENT AND RESOURCE SHARING

Further information and requests for resources and reagents should be directed to and will be fulfilled by the Lead Contact Tobias Bollenbach (t.bollenbach@uni-koeln.de).

EXPERIMENTAL MODEL AND SUBJECT DETAILS

Strains, Antibiotics, and Culture Conditions

We used the promoter-GFP library parent *E.coli* K-12 strain MG1655 as wild-type, unless stated otherwise. Deletion strains, i.e. Δ*guaB*, Δ*purA*, Δ*nuoC*, Δ*rpoS*, and all strains listed below, are from the KEIO collection (Baba et al., 2006) with parent strain BW25113, unless stated otherwise.

All experiments were performed in minimal M9 medium (1x M9 salts, 2mM $MgSO_4$, 0.1mM $CaCl_2$, supplemented with 4g/L glucose and 1g/L amicase, pH ~7.1). For experiments in 96-well plates, Triton X-100 was added at 0.001% (v/v) to reduce surface tension in the microplate wells; this had no detectable effect on growth or gene expression. Inosine, guanine, adenine and thymine were added at 0.3mM. Antibiotics for dynamic measurements were dissolved in ethanol (TMP, TET, CHL) or in dimethylformamide (NIT) and added from concentrated stocks (stored at −20°C in the dark) at the indicated concentrations. Antibiotics for selection and glycerol stocks were dissolved in water; kanamycin was used at 25μg/mL; ampicillin at 50μg/mL; spectinomycin at 100μg/mL. For the acid stress experiment (Figures 2, 3, S2, and S4), the pH of the M9 medium without TMP was adjusted to pH 3 with hydrochloric acid (HCl). For the formic acid experiment (Figures 1E and S1D), the pH of the M9 medium was titrated to pH 6.4. All chemicals were obtained from Sigma-Aldrich except when stated otherwise.

For monitoring *gadBC* expression in deletion mutants, KEIO strains were transformed with the plasmid pUA139 P_{gadB}-*gfp* Amp^R (Key Resources Table). Specifically, the following strains were checked:

aceA, *aceB*, *aceF*, *acnB*, *acrB*, *adhE*, *adiA*, *aldA*, *appB*, *appC*, *aqpZ*, *atpB*, *atpC*, *atpD*, *atpE*, *atpG*, *atpH*, *atpI*, *cadA*, *cbpA*, *cfa*, *clcA*, *codB*, *cydB*, *cydX*, *cyoA*, *cyoB*, *cyoC*, *cyoD*, *cyoE*, *dkgA*, *dkgB*, *dld*, *dnaK*, *dps*, *eutD*, *fdhF*, *focA*, *frdA*, *fre*, *gabT*, *gadB*, *gadC*, *gadE*, *gadW*, *galE*, *gcvP*, *gdhA*, *gldA*, *gloA*, *gloB*, *gltP*, *gor*, *gpmM*, *gshA*, *gshB*, *guaB*, *hchA*, *hdeA*, *hmp*, *hycA*, *hycB*, *hycC*, *hycD*, *hycE*, *hycF*, *hycG*, *hycH*, *hycI*, *icd*, *ilvA*, *ilvC*, *ilvE*, *kbl*, *kdpF*, *kefB*, *kefC*, *kefF*, *kefG*, *ldcC*, *ldhA*, *lldD*, *ltaE*, *lysC*, *maeB*, *marA*, *marR*, *mdh*, *mgsA*, *mhpF*, *miaB*, *mnmE*, *mnmG*, *mscK*, *nadR*, *narG*, *ndh*, *ndk*, *nfsB*, *nrdD*, *nrdE*, *nrdF*, *nuoA*, *nuoB*, *nuoC*, *nuoE*, *nuoF*, *nuoG*, *nuoH*, *nuoI*, *nuoJ*, *nuoK*, *nuoL*, *nuoM*, *nuoN*, *ompC*, *ompF*, *pflB*, *phoB*, *phoE*, *pntA*, *pntB*, *potE*, *pta*, *ptsG*, *purC*, *purM*, *purT*, *puuD*, *puuE*, *pykF*, *rcsB*, *relA*, *rpoS*, *rsxA*, *sdhA*, *sdhB*, *sdhC*, *sdhD*, *serA*, *slp*, *soxS*, *speF*, *sthA*, *talA*, *tdcB*, *tdh*, *thrA*, *thrB*, *thrC*, *tolC*, *tynA*, *wrbA*, *ydbD*, *yaeE*, *yeiG*, *yghZ*, *yiaY*, *yqiL*, *zwf*

For the experiment using a simpler protocol to measure population-level gene expression in response to TMP (Figure S1B), the following promoters from the promoter-GFP library were analyzed:

acnB, *ada*, *ahpC*, *ansA*, *araC*, *arcB*, *aroP*, *ascG*, *atpI*, *b0360*, *brnQ*, *clpP*, *clpX*, *crp*, *cspG*, *cyaA*, *cyoA*, *cysJ*, *cysK*, *cytR*, *dcm*, *deoC*, *dnaK*, *dnaQ*, *dps*, *dsbG*, *exuR*, *fhuF*, *flgM*, *fliY*, *focA*, *folA*, *fpr*, *fruB*, *ftsK*, *fur*, *gadA*, *gadB*, *gadW*, *gadX*, *gcvP*, *glnA*, *glnH*, *glnL*, *glpX*, *gmk*, *groE*, *grxB*, *grxC*, *gshA*, *gss*, *guaB*, *gyrB*, *hdeA*, *hdeD*, *hemC*, *htpG*, *ihfB*, *ileX*, *insA_3*, *intZ*, *kefG*, *lacI*, *ldhA*, *leuS*, *lexA*, *lon*, *maeB*, *mngR*, *msrB*, *napF*, *ndk*, *nfnB*, *nfo*, *nhaA*, *nhoA*, *nrdH*, *ompC*, *ompR*, *ompX*, *osmE*, *oxyR*, *pck*, *pfkB*, *pgi*, *pstS*, *pth*, *ptsG*, *purT*, *pykF*, *rdoA*, *recA*, *rluE*, *rmuC*, *rob*, *rpoE*, *rpoH*, *rpsT*, *rrnD*, *ruvA*, *sbmC*, *sdaA*, *sdhC*, *serA*, *slp*, *sodA*, *sodB*, *sodC*, *speE*, *sppA*, *ssb*, *sscR*, *talA*, *talB*, *tktA*, *tnaC*, *tolC*, *torR*, *trmU*, *trpL*, *trxA*, *tyrS*, *ubiG*, *ung*, *uvrA*, *uvrY*, *wrbA*, *yacG*, *yafD*, *yafK*, *yafL*, *yafV*, *yagB*, *yaiA*, *ybeB*, *ybfE*, *ybgA*, *ybgC*, *ybgI*, *ybhL*, *ybiS*, *ybjC*, *ybjS*, *ybjX*, *ycbZ*, *ycgJ*, *ycgL*, *ychF*, *ycjK*, *ydbH*, *ydeO*, *ydgK*, *ydgL*, *ydhZ*, *ydiY*, *yeaH*, *yeaT*, *yedW*, *yehS*, *yggD*, *yggE*, *ygjD*, *ygjH*, *yhaH*, *yhfA*, *yhiD*, *yhjK*, *yihN*, *yiiU*, *ykgI*, *yliE*, *yncG*, *yqjC*, *yrbA*

We sequenced 50 plasmids from our copy of the promoter-GFP library and did not find the indicated promoters in some cases (*pitB*, *aqpZ*, *pheL*, *dps*, *b1997*, *yhcF*). Their promoter names were replaced with the correct names of the promoters as found in these plasmids (*gadA*, *dps*, *serA*, - , *aidB*, *aidB*), respectively, in Tables S1 and S2 and throughout the paper.

METHOD DETAILS

Gene Expression Measurements with Robotic System

Cultures were diluted ~1:1000 (with a VP408 pin tool, V&P Scientific, Inc.) from M9 medium glycerol stocks containing kanamycin into fresh M9 medium without antibiotic. All reporter library strains were grown in 200μL in transparent flat-bottom 96-well plates (Nunc) at 30°C with rapid shaking. Absorbance at 600nm (A_{600}) and GFP fluorescence (excitation 485nm(20), emission 535nm (25)) were measured every ~25 minutes using an automated robotic system (Tecan Freedom Evo150) and a plate reader (Tecan infinite 500). Whenever the absolute absorbance (A_{600}) of 0.13 (which corresponds to a background corrected A_{600} of ~0.093) was exceeded, the cultures were diluted 10-fold into fresh M9 medium using a 96-channel pipetting head (Figure 1B). After the first dilution, 2μL of antibiotic stock adjusted to 100-fold the desired concentration was added to all wells when they exceeded an absorbance threshold of 0.08 (background corrected A_{600} ~0.043). The subsequent dilutions were done into medium containing antibiotics at the same concentration.

Plasmid Construction

The plasmid pUA139 P_{gadB}-*gfp* Amp^R (Key Resources Table; used in Figures S1C and S6A) was constructed by amplifying P_{gadB} from the MG1655 chromosome using the primers CGGGATCCTCCTGCAGCATGGACTGAG and CCGCTCGAGCATTTTCGTCGT CCCAGGTC (underlined bases are restriction sites). Kan^R on pUA139 was exchanged by Amp^R amplified from the plasmid pZS11-*pHluorin* (Key Resources Table) using the primers GCGAGCTCGTAAACTTGGTCTGACAGTTAC and CGGGATCCTCAG GTGGCACTTTTCGG.

The plasmid pZS11-*pHluorin* (Key Resources Table; used in Figures 3G, 3H, 5C, S4, S5, and S6C) was constructed by amplifying the ratiometric *pHluorin* (Martinez et al., 2012) with the primers GGCCGAATTCATTAAAGAGGAGAAAGGTACCGCATGAGTAAAG GAGAAGAACTTTTCACTGG and GGCCAAGCTTTTATTTGTATAGTTCATCCATGCCATG and putting it on a low-copy number plasmid (pSC101 origin) under a constitutive $P_{LtetO-1}$ promoter without the Tet repressor present (Lutz and Bujard, 1997).

The plasmid pZS41-*mCherry* (Key Resources Table; used in Figures 2, 3B–3F, 4A, 4D, 5B, S2, S3, and S5A), used for segmentation, was cloned from the plasmid containing the constitutive $P_{LtetO-1}$ promoter with absent Tet repressor (Lutz and Bujard, 1997) and the plasmid pZS2-123 (Cox et al., 2010) which contains the fluorescent protein *mCherry*.

Strain Construction and Verification

The Δ*guaB* and Δ*purA* strains were verified phenotypically (i.e. dependence on purine base supplementation) and genotypically by PCR using the primers CGCCGGAAAGAATAATGCCG and CAGTCGATAGTAACCCGCCC for Δ*guaB*, and GTTTTGGCGGTG GACTTGTG and TCAGCGCACGTAATCCGTAA for Δ*purA*; the *ΔnuoC* strain was PCR-verified using primers CACCACGGAC CATTTGCAATG and CAGTCATAGCCGAATAGCCT (binding inside the kanamycin resistance); the Δ*rpoS* strain was PCR-verified using the primers ATTACCTGGTGCGTATGGGC and GAAATCCGTAAACCCGCTGC; the strain MG1655 Δ*rpoS* was obtained from the respective KEIO strain by P1 transduction (Lennox, 1955) and PCR-verified with the same primers.

To obtain chromosomally integrated promoter-reporter fusions, we devised an efficient method to easily accept various promoters from the set of plasmids used in (Zaslaver et al., 2006); this method will be described in detail elsewhere. In short, we used lambda-red recombineering as described in (Datsenko and Wanner, 2000) to integrate PCR products derived from the promoter-GFP library (Zaslaver et al., 2006) into the *intS* locus (chromosome positions 2,466,545 -> 2,467,702; (Keseler et al., 2013)) on the chromosome. First, a sequence containing the fluorescent protein and the biggest part of the kanamyin resistance was integrated into the *intS* locus. Then, PCR products from the promoter-GFP library were amplified using the primers GCGATACCGTAAAGCACGAG (MKan-1) and TTCTTCACCTTTGCTCATATGTATATCTCC and integrated into this sequence. Through our method, the GFPmut2 from the reporter plasmid library was replaced by a YFP variant from the plasmid pZS2-123 (Cox et al., 2010). Since we detected a mutation in the *gadB* library plasmid, this promoter was first amplified from the chromosome with primers CGGGATCCTCCTGCAGCATGGAC TGAG and CCGCTCGAGCATTTTCGTCGTCCCAGGTC and cloned into the library backbone (underlined bases are restriction sites). Recombineering was performed with the plasmid pSIM19 (Datta et al., 2006). All integrated constructs were validated by sequencing the PCR product obtained with primers upstream and downstream of *intS*, respectively: GTACTTACCCCGCACTCCAT and TGTTCAGCACACCAATAGAGG on the chromosomal DNA. This protocol yielded the strains Δ*intS*::P_{gadB}-*yfp* (Key Resources Table; used in Figures 3B–3F and 4D), Δ*intS*::P_{wrbA}-*yfp*, Δ*intS*::P_{dps}-*yfp*, and Δ*intS*::P_{folA}-*yfp* (Key Resources Table; all used in Figure S3).

To obtain the strains BW25113 Δ*guaB*Δ*intS*::P_{gadB}-*yfp* (Key Resources Table; used in Figure 5B), BW25113 Δ*purA*Δ*intS*::P_{gadB}-*yfp* (Key Resources Table; used in in Figure 5B), and MG1655 Δ*rpoS*Δ*intS*::P_{gadB}-*yfp* (Key Resources Table; used in Figure 3C) the kanamycin resistance cassette was first deleted as previously described (Datsenko and Wanner, 2000) using plasmid pCP20 (Cherepanov and Wackernagel, 1995) before lambda-red recombineering. P_{gadB}-*yfp* was amplified from the MG1655 Δ*intS*::P_{gadB}-*yfp* strain (Key Resources Table; used in Figures 3B–3F and 4D) and integrated using the primers GTACTTACCCCGCACTCCAT and TGTTCAGCA CACCAATAGAGG. To obtain the strain Δ*intS*::P_{gadB}-*mCherry* (Key Resources Table; used in Figure 3H), we replaced the sequence of *gfp* in the plasmid with P_{gadB}-*gfp* by *mCherry* amplified from pZS41-*mCherry* using the primers CCGCTCGAGAGATCCTCTA GATTTAAGAAGGAGATATACATATGGTTTCCAAGGGCGAGGAGG and GCGCCTAGGTCTAGGGCGGCGGATTTGTCCTACTC, followed by recombineering with the primers MKan-1 and CTACTCAGGAGAGCGTTCACC. We also validated all strains with respect to their growth rate, gene expression in response to TMP, and dose-response to kanamycin.

Microfluidics and Time-Lapse Microscopy

For all microscopy experiments, we used a microfluidics device in which bacteria grow in microcolonies. This device allows switching between different inlets, and equilibration to the new condition happens within minutes (CellASIC ONIX, Merck Millipore). Bacteria were inoculated from frozen glycerol stocks at a dilution of 1:1000 to 1:5000 and grown to an optical density (OD_{600}) of 0.05 to 0.1. Then they were diluted 1:100 and loaded into the microfluidics chamber which was preheated to 30°C. This normally led to spatially well separated single cells in the microfluidics chamber. All experiments were performed in a heated chamber at 30°C. Data acquisition started 1-2 hours after loading. Images were taken every 10 to 20 minutes using a 100x oil objective with an EMCCD camera (Hamamatsu) on a Nikon Eclipse Ti-E with a LED light engine (Lumencor). Excitation wavelengths for YFP were CWL/FWHM 513/17nm and emission wavelengths were dichroic LP 520nm, CWL/BW 542/27nm, respectively. Maturation times of GFP and YFP were below 10 minutes in our conditions, measured by the accumulation of fluorescent protein after translational inhibition with CHL in Isopropyl β-D-1-thiogalactopyranoside (IPTG)-inducible $P_{LlacO-1}$ -fluorescent protein strains (Lutz and Bujard, 1997), as described in (Megerle et al., 2008). In contrast, mCherry had a longer maturation time (~32 min) and was therefore mostly used as a segmentation color.

Measurements of Intracellular pH

For all measurements of intracellular pH, the plasmid pZS11-*pHluorin* was transformed into the strain of interest. For calibration, we used a medium that could be buffered to different pH values (which was not possible with the phosphate buffered M9 minimal medium). We used M63 medium (M63 salts, 1mM $MgSO_4$, 4g/L glucose, 1g/L amicase) buffered to different pH values (pH 8.5 with N-Tris(hydroxymethyl)methyl-3-aminopropanesulfonic acid (TAPS), pH 7.5 with 3-(*N*-Morpholino)propanesulfonic acid (MOPS), pH 6.5 with 1,4-Piperazinediethanesulfonic acid (PIPES), each 50mM), and supplemented with 40mM potassium benzoate and 100mM methylamine hydrochloride for collapsing the intracellular pH (uncoupling) and pH adjusted with hydrochloric acid and potassium hydroxide. Due to the high proton concentrations at low pH values (pH 3 to pH 5), buffering was not necessary and calibration could be done using normal M9 medium titrated to the desired pH with hydrochloric acid and 40mM potassium benzoate for uncoupling. Calibration was performed in the microfluidics system by switching between the different inlets (with medium at different pH). After a switch, the new fluorescence ratio was reached after a few minutes and we imaged every 5 min over a period of 20-30 min (Figure S4A). Excitation wavelengths for *pHluorin* were 390/18 nm and 438/24 nm and emission LP 495 nm, BP 520/35 nm. Excitation at 438/24 nm yielded the same results as excitation at 475/28 nm, close to the wavelength used in (Martinez et al., 2012). Calibration was done for each experiment separately due to slight day-to-day changes in microscope illumination. Typical absolute pH values in exponentially growing cells varied between experiments (pH 8 to pH 8.5), probably due to slight variations in uncoupling efficiency and decreased sensitivity of *pHluorin* at higher pH values. After the addition of hydrochloric acid (Figures 3G and 3H), repeated measurements of the same cell had a much smaller variability (coefficient of variation ~3%) than measurements of different cells (coefficient of variation ~12%). The coefficient of variation for the ratio (not translated into pH) before and after the addition of HCl was 5% and 12%, respectively. Fluorescence levels right after HCl addition dropped due to the pH dependence of YFP (Figure 3D).

QUANTIFICATION AND STATISTICAL ANALYSIS

Analysis of the Population-Level Data

All data analysis was performed using custom MATLAB (MathWorks, version R2011b) code. Absorbance background was measured before each experiment in each plate (filled with 200μL M9 medium per well) before inoculation and subtracted in a well-specific manner. GFP background subtraction was done as described (Zaslaver et al., 2006). Only promoters with a mean signal-to-noise ratio (GFP/A_{600} divided by the SD of GFP/A_{600} from the two promoter-less strains on each library plate) greater than 5 and exclusively positive GFP/A_{600} values were analyzed, reducing the number of promoters to ~1,000 (1,157 for TMP, 1,052 for TET, 851 for NIT, 934 for CHL; Table S1). Parts of growth curves that clearly suffered from technical problems (e.g. due to air bubbles in the well), were exchanged with the same part of the closest growth curve from another strain; this was unproblematic as nearly all strains from the library grew at the same rate in our conditions.

After each of the four 10-fold dilution steps in our protocol (Figure 1B), the background subtracted absorbance and GFP values dropped to ~1/10 of the value before the dilution (Figure 1B). This resulted in meaningless values at the point of dilution when differentiating the whole measurement curve. As we needed these differentiated data for later normalization and correction of the data (see below), we compensated for this drop in absorbance and GFP values by adding an offset to all the measurements after each dilution. This offset was determined by calculating a linear fit (using the MATLAB function *robustfit*) to the 4 log-absorbance values measured before the dilution, and extrapolating it to the next time point. Further, using our protocol with recurring dilutions and the addition of antibiotics, it was impossible to keep the measurement intervals at exactly 25 minutes at all times. In order to have a common time axis for all measurements, we interpolated all measured A_{600} and GFP data onto a time axis with the fixed interval of 25 minutes, counting forward in time after the time point when antibiotics were added, and backwards in time before. This was unproblematic, as the real measurement points were close to 25 minutes for all data. All data were subsequently smoothed with a moving average filter with a span of 3 (using the MATLAB function *smooth*) and time series were cropped before entry into stationary phase.

Using our plasmid-based GFP reporter system, nonspecific effects can occur (like plasmid copy number changes (Bollenbach et al., 2009)) affecting all strains in a similar way. We corrected for these nonspecific effects in our data using the following procedure. The total cellular protein concentration and, to a good approximation, the median GFP concentration over all measured strains behaves as

$$\frac{d\widetilde{GFP}}{dt} = \widetilde{PA} - \mu \cdot \widetilde{GFP},$$

where $\widetilde{PA}$ is the median promoter activity over all strains, obtained from the individual strain promoter activity $PA = \frac{\frac{\Delta GFP}{\Delta t}}{A_{600}}$, where A_{600} is the absorbance value at the later time point of Δt. Further, μ is the growth rate and $\widetilde{GFP}$ is the median GFP concentration over all strains. Based on the assumption that the total cellular protein concentration does not change over time (Basan et al., 2015), the median promoter activity $\widetilde{PA}$ is directly proportional to the growth rate μ:

$$\widetilde{PA} = \mu \cdot \widetilde{GFP}$$

For each experimental condition, we corrected our data for deviations from this equation by subtracting the difference between $\log_2(\widetilde{PA})$, shifted to zero for t = 0 and $\log_2(\mu)$, also shifted to 0 for t = 0, from the promoter activity PA of each strain. From this corrected

PA of each strain, we calculated back the GFP concentration by multiplication with the absorbance values and numerical integration using the MATLAB function *trapz*. To compare relative changes in gene expression upon drug addition, all GFP/A_{600} data were $\log_2$-transformed and shifted to zero for t = 0. All data shown in Table S1 were normalized in the described way.

For the simpler experiment, in which TMP was added from the beginning, we divided the corrected GFP/A_{600} averaged between A_{600} of 0.01 and 0.1 in the TMP stressed data by the non-stressed control to obtain fold-changes. The $\log_2$ transformed fold-change of each promoter was then subtracted by the median over all $\log_2$ transformed fold-changes to correct for nonspecific effects.

Information on gene regulation was from (Gama-Castro et al., 2011; Keseler et al., 2013; Seo et al., 2015) (Table S2). Maximum fold-change in expression was determined as the maximum (for upregulated promoters) or minimum (for downregulated promoters) GFP/A_{600} change on a $\log_2$ scale after the addition of stress. Response times were determined as the time until the half maximum expression on a $\log_2$ scale was reached (Figure 1C). Instantaneous growth rates in Figures 1B, 4B, S1A, S1D, and S6B were determined by dividing the difference between subsequent log-transformed absorbance measurements by the respective time interval for each strain and averaging over all measured strains.

Analysis of Single-Cell Data

Time-lapse microscopy movies were segmented and analyzed using an adapted version of the MATLAB program 'SchnitzCells' (Young et al., 2012). Fluorescence background of the surrounding environment was subtracted as the median fluorescence over all pixels outside bacteria. Expression level was determined by dividing the total fluorescence signal from a cell by its total area. For the strain MG1655 Δ*rpoS*Δ*intS*::P_{gadB}-*yfp*, we subtracted the autofluorescence background as the mean expression from a microcolony without YFP present due to low expression. When cells lysed, their fluorescence dropped sharply. Survival time was therefore determined as the last time point at which fluorescence intensity of the segmentation color (*mCherry* or *pHluorin*) was still above the detection threshold. Photobleaching was negligible under our conditions (~1% per frame; determined by imaging a microcolony with 10 s time interval). Bootstrap SE in Figures 3 and S3 was calculated using MATLAB function *bootstrp*, with n = 1000. All single cell data presented in this paper are either from one microcolony or pooled from several microcolonies. The results coming from one microcolony are representative of the results of at least two microcolonies; results obtained by pooling data from several microcolonies were not affected by extreme data from one specific microcolony. Information on the exact number of single cells and microcolonies analyzed are provided in the figure legends. In general, all microcolonies that had high image quality and little spatial movement of cells were analyzed.